Biological Cybernetics
https://doi.org/10.1007/s00422-018-0773-y

Biological Cybernetics

ORIGINAL ARTICLE

A planar neuro-musculoskeletal arm model in post-stroke patients

Mehran Asghari[1] · **Saeed Behzadipour**[1,2] · **Ghorban Taghizadeh**[3,4]

Received: 3 January 2018 / Accepted: 20 July 2018

Abstract
Mathematical modeling of the neuro-musculoskeletal system in healthy subjects has been pursued extensively. In post-stroke patients, however, such models are very primitive. Besides improving our general understanding of how stroke affects the limb motions, they can be used to evaluate rehabilitation strategies by computer simulations before clinical evaluations. A planar neuro-musculoskeletal arm model for post-stroke patients is developed. The main idea is to use a set of new coefficients, Muscle Significance Factors (MSF), to incorporate the effects of stroke in the muscle control performance. The model uses the optimal control theory to mimic the performance of the CNS and a two-link skeletal model with six muscles for the biomechanical part. The model was developed and evaluated using experimental data from six post-stroke patients with Brunnstrom levels of 4–6. The results show that MSFs are relatively distinct and independent from the arm motion which is used to determine their values. Its variation is in the range of 0–2.58% and decreases in higher Brunnstrom levels. The mean error of the model in predicting the path of motion varies from 0.9% in level 6 to 5.58% in level 4 subjects which can be considered a promising level of accuracy. Using the proposed model and the MSF to customize the model for each individual stroke patient seems a promising approach. It shows a reasonable level of robustness, i.e., independence from the type of motions and correlated with the severity of stroke, and accuracy in predicting the shape of the motion path.

Keywords Optimal control · Musculoskeletal model · CNS model of stroke patients · Neuro-musculoskeletal arm model

1 Introduction

Mathematical models of the central nervous system (CNS) has been increasingly used to provide better understanding of goal-directed movements (Shadmehr et al. 2010). Such models tend to simulate human motor system in order to find and analyze the strategies of CNS during biological motions (Flash and Hogan 1985; Stroeve 1998; Suzuki et al. 1997; Uno et al. 1989), to design motion for robots (Dong et al. 2015; Mombaur et al. 2010) and to evaluate the function and response of the CNS after stroke (Han et al. 2008; Reinkensmeyer et al. 2003; Zadravec and Matjačić 2013). Since the function of the CNS depends on the musculoskeletal system of the body, such models tend to include both neural and musculoskeletal systems (Todorov and Li 2003).

Planar arm movements, on a transverse plane at the shoulder's height, have been the focus of several works (Bernabucci et al. 2007; Bhushan and Shadmehr 1999; Sharifi et al. 2017; Thaler and Todd 2009; Zadravec and Matjačić 2013) due to the relatively simple kinematics and muscular system. In such models, a 2DOF-musculoskeletal model is built and integrated with a mathematical representation of the CNS. The resulting trajectories (calculated by the model) are then compared with the experimental ones.

Two main approaches have been introduced in the literature to model the CNS in motion planning: (1) knowledge-based techniques in which means of intelligent systems such as Artificial Neural Networks (ANN) (Blana et al. 2009; Park

Communicated by Benjamin Lindner.

✉ Saeed Behzadipour
behzadipour@sharif.ir

Mehran Asghari
mehran.asghari322@yahoo.com

Ghorban Taghizadeh
gh_taghizade@yahoo.com

1 Mechanical Engineering Department, Sharif University of Technology, Tehran, Iran

2 Djavad Mowafaghian Research Center in Neurorehabilitation Technologies, Tehran, Iran

3 Department of Occupational Therapy, School of Rehabilitation Sciences, Iran University of Medical Sciences, Tehran, Iran

4 Rehabilitation Research Center, School of Rehabilitation Sciences, Iran University of Medical Sciences, Tehran, Iran

Published online: 28 July 2018

and Durand 2008; Stroeve 1998) are trained by experimental data to learn the behavior of the CNS, and (2) Control theory approaches in which a unified control logic is assumed for the CNS independent from the type of motion (Flash and Hogan 1985; Li and Todorov 2007; Sharifi et al. 2017; Uno et al. 1989; Zadravec and Matjačić 2013). The first approach requires large amount of experimental data for training the model; furthermore, the validity is limited to the tasks by which the model is trained.

Optimal control, on the other hand, is an example of the second approach (Flash and Hogan 1985; Li and Todorov 2007; Sharifi et al. 2017; Uno et al. 1989; Zadravec and Matjačić 2013) in which, the working logic of the CNS is assumed to be optimizing a cost function while designing a limb motion. The theory is more than half a century old and formulated in the framework of optimal control theory in 2002 (Todorov and Jordan 2002). It has attracted much attention in the community and been frequently used for constructing models of biological movements, and motor control (Flash and Hogan 1985) and has provided a fruitful general framework for the CNS modeling (Todorov and Li 2003).

Several different cost functions have been proposed to be minimized by the CNS in human movements. For instance, Anderson and Pandy (2001) used metabolic energy as a cost function for gait generation, Lee et al. (2009) used maximal muscle activity to evaluate a musculoskeletal rehabilitation program. Heim and Stryk tried to optimize the trajectory of a robotic arm for a time and energy-optimal motion (Heim and Stryk 2000). In arm reaching movements, motivated by empirical investigations, two criteria have been used for the cost function: minimum joint torque (Uno et al. 1989; Zadravec and Matjačić 2013; Li and Todorov 2007), and minimum fatigue or muscle stress (Dong et al. 2015; Sharifi et al. 2017). The second criterion has a better biological explanation and generates more accurate results (Sharifi et al. 2017).

Although there are several mathematical models that describe the normal human's CNS in motion planning, only a few have tackled the post-stroke subjects. As far as the authors know, there has been no CNS model based on the optimal control criterion for the post-stroke patients. However, musculoskeletal deficits due to stroke have been investigated in some studies in this area. Matjaz developed an optimal control on the human arm model, which could simulate arm tightness after stroke (Zadravec and Matjačić 2013). He supposed a rate for increasing the stress of human muscles in stroke.

Modeling the CNS in post-stroke has been done by some researchers using tools of intelligent systems such as ANN's. Such works, however, has targeted only the general characteristics of such patients (Çelik et al. 2014) or studied a general hypothesis (Han et al. 2008). For instance, Han and his colleagues developed a computational model to show that if the amount of motor training after stroke passes a particular threshold, the motor performance reinforces itself spontaneously (Sharifi et al. 2017). As another example, Reinkensmeyer et al. used a population vector model to show how the reaching accuracy is affected by the amount of killed cells in stroke (Thaler and Todd 2009). One should note that since neurons die haphazardly in stroke (Han et al. 2008; Reinkensmeyer et al. 2003), the location and size of the lesion substantially affect the CNS function. As a result, the above-mentioned models are either intrinsically not suitable for subject-specific studies or require large amount of experimental data from each subject for training purposes.

In this paper, we propose a patient-specific planar neuromusculoskeletal model for the post-stroke patients which is an extension to the models using the optimal control theory for the CNS. The core hypothesis behind the present model is that the CNS, after stroke, still tries to apply its optimal control criterion; however, since some neural connections to the musculoskeletal system are severed, the motion planning provides different results. This was included in the model by assigning a muscle significance factor, MSF, to each muscle which determines its weight (significance) in the cost function of the optimal controller and is determined experimentally. The model was then evaluated by comparing its predictions for the arm motion path with the actual movements of some stroke patients.

2 Method

The overall scheme of the proposed model is shown in Fig. 1. The stroke model, in the middle of the block diagram, consists of two interacting parts: a planar musculoskeletal arm model, and an optimal controller as the CNS. In order to tune the model for each individual subject, a training loop was used. The subject was asked to move his affected hand from a given starting point to a target one on the plane of motion. The same points were given to the model and the resulting path from the model was subtracted from the experimental one to calculate the error. The error between the two paths was then minimized through an optimization routine in which, certain parameters of the stroke model (i.e., MSF) were tuned. The tuned model was then validated by other experimental movement data of the same patient. The details of each part are given in the following sections.

2.1 Musculoskeletal arm model

The schematic of the musculoskeletal arm model is shown in Fig. 2 (Sharifi et al. 2017). The model was earlier used in several studies and shown to provide an acceptable approximation of arm and shoulder in planar movements (Balaghi et al. 2016; Blana et al. 2009; Breteler et al. 1999; Sharifi et al. 2017; Zadravec and Matjačić 2013). The model has 2 links

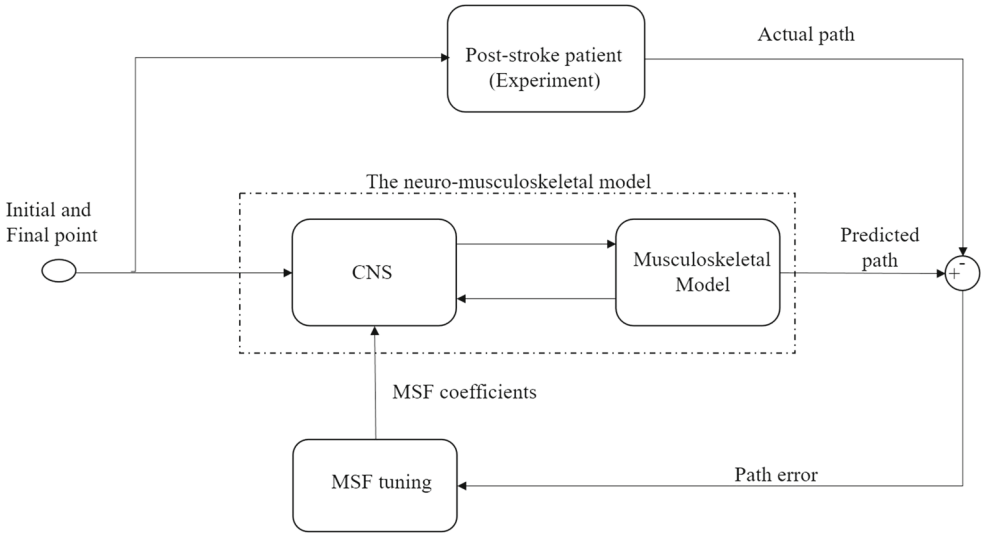

Fig. 1 Neuro-musculoskeletal model of stroke and the parameter tuning procedure

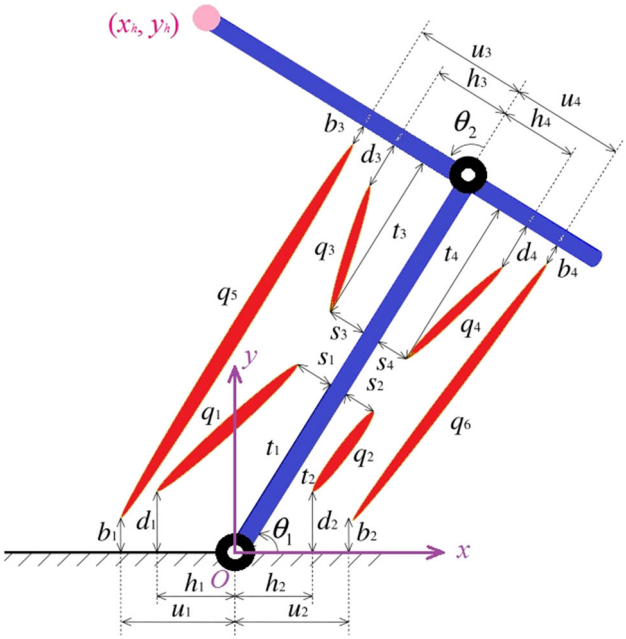

Fig. 2 Planer musculoskeletal arm model with six muscles and 2 links. (Reproduced with permission from Sharifi et al. 2017)

(a link for the forearm and another one for the upper arm), two joints (shoulder and elbow) providing two degrees of freedom. Six muscles were considered. Four mono-articular muscles: pectoralis major, posterior deltoid, brachialis, lateral head of triceps brachii, and two bi-articular muscles: biceps brachii, long head of triceps.

The 2D motion of the arm was assumed to occur on a horizontal plane at the height of the shoulder and the gravity was neglected. As for the model parameters, the configuration of muscles and their attachments to the segments were taken from (Pigeon et al. 1996; Veeger et al. 1997), the physiological cross-sectional area of each muscle is based on (Holzbaur et al. 2007; Murray et al. 2000), mass and inertia parameters, as functions of the lengths of arm and forearm, and the constants of the viscosity matrix were extracted from (Nakano et al. 1999; Suzuki et al. 1997).

The dynamic equations of the skeletal model, using the Lagrange's method are:

$$\mathbf{M}(\boldsymbol{\theta})\ddot{\boldsymbol{\theta}} + \mathbf{D}\left(\boldsymbol{\theta}, \dot{\boldsymbol{\theta}}\right) = \boldsymbol{\tau} \tag{1}$$

where $\boldsymbol{\tau} = [\tau_1, \tau_2]^{\mathrm{T}}$ is the joint torque vector, $\boldsymbol{\theta} = [\theta_1, \theta_2]^{\mathrm{T}}$ is the joint angle vector, $\mathbf{M}(\boldsymbol{\theta})$ is the mass matrix, and $\mathbf{D}\left(\boldsymbol{\theta}, \dot{\boldsymbol{\theta}}\right)$ includes the Coriolis, centrifugal and viscous friction. They were expressed in terms of the geometry, mass and mechanical properties of the model components as:

$$\mathbf{D}\left(\boldsymbol{\theta}, \dot{\boldsymbol{\theta}}\right) = \begin{bmatrix} -a_2\left(2\dot{\theta}_1\dot{\theta}_2 + \dot{\theta}_2^2\right)\sin(\theta_2) + k_1\dot{\theta}_1 \\ a_2\dot{\theta}_1^2\sin(\theta_2) + k_2\dot{\theta}_2 \end{bmatrix} \tag{2}$$

$$\mathbf{M}(\boldsymbol{\theta}) = \begin{bmatrix} a_1 + 2a_2\cos(\theta_2) & a_3 + a_2\cos(\theta_2) \\ a_3 + a_2\cos(\theta_2) & a_3 \end{bmatrix} \tag{3}$$

$$\begin{aligned} a_1 &= m_1 l_{g1}^2 + I_1 + m_2\left(L_1^2 + l_{g2}^2\right) + I_2 \\ a_2 &= m_2 L_1 l_{g2} \\ a_3 &= m_2 l_{g2}^2 + I_2 \end{aligned} \tag{4}$$

where L_1 is the length of the upper arm and k_i, m_i, I_i, l_{gi} indicate the viscous friction coefficients for the shoulder and elbow joints, mass, the moment of inertia and the location of the center of mass for the upper arm and forearm, respectively.

The joint torque in Eq. (1) can be expressed in terms of muscle forces according to the relation between the muscle

and joint space in the musculoskeletal model. For this purpose, the muscle lengths vector $\mathbf{Q} \in \mathbb{R}^6$ was first expressed in terms of the joint angles, $\boldsymbol{\theta} = [\theta_1, \theta_2]^{\mathrm{T}}$ (Sharifi et al. 2017). If the kinematic constraints imposed by the muscle lengths are expressed as:

$$\mathbf{F}_{6\times1}(\mathbf{Q}_{6\times1}, \boldsymbol{\theta}_{2\times1}) = 0$$

Then, the differentials are related as:

$$\frac{\partial \mathbf{F}}{\partial \mathbf{Q}}\delta\mathbf{Q} + \frac{\partial \mathbf{F}}{\partial \boldsymbol{\theta}}\delta\boldsymbol{\theta} = 0$$

Which results in:

$$\delta\mathbf{Q} = \mathbf{J}(\boldsymbol{\theta})\delta\boldsymbol{\theta} \tag{5}$$

where $\mathbf{J} = -\left(\frac{\partial \mathbf{F}}{\partial \mathbf{Q}}\right)^{-1}\left(\frac{\partial \mathbf{F}}{\partial \boldsymbol{\theta}}\right)$ indicates the Jacobian matrix for the muscle extending velocities with respect to the joint angular velocities. As a result, the relation between the muscle contractile forces and the joint torques was directly established using the virtual work principle:

$$\boldsymbol{\tau} = -\mathbf{J}^{\mathrm{T}}(\boldsymbol{\theta})\boldsymbol{\alpha} \tag{6}$$

where $\boldsymbol{\alpha} \in \mathbb{R}^6$ is the muscular tensile force vector and determined by the central nervous system. In order to use the model in the optimal control problem, Eq. (1) should be expressed in state space, so state vector $\mathbf{x} = [x_1, x_2, x_3, x_4]$, where $x_1 = \theta_1, x_2 = \theta_2, x_3 = \dot{\theta}_1, x_4 = \dot{\theta}_2$ was used.

2.2 CNS model for stroke

An optimal controller was used to model the CNS. This controller determines the muscle tensile forces $\boldsymbol{\alpha}$ such that a cost function is minimized while particular starting and ending point constraint as well as the dynamics of the arm are satisfied. The cost function, in this work, is the muscle stress (Sharifi et al. 2017), which is considered as the summation of squares of stress of muscles integrated over the entire motion:

$$g = \frac{1}{2}\int_0^{t_f} \mathbf{S}^{\mathrm{T}}(t)\mathbf{S}(t)\mathrm{d}t \tag{7}$$

where $\mathbf{S}(t) = \left[\frac{\alpha_1(t)}{P_1}, \frac{\alpha_2(t)}{P_2}, \ldots \frac{\alpha_6(t)}{P_6}\right]^{\mathbf{T}}$ is the muscle stress vector, in which P_i is the muscle cross-sectional area and $\alpha_i(t)$ is the muscle tensile force. Also, t_f is the time of movement, which is measured from the onset of movement to the moment the hand reaches the target point.

To solve this, particular state constraints needed to be considered. The initial and final velocities were set to zero. All muscles were assumed to bear tensile stress only and the maximum force was restricted and obtained from the product of muscle cross-sectional area and the maximum muscle tensile stress which was considered to be $\boldsymbol{\sigma}_{\mathrm{Max}} = 0.6$ Mp (Sharifi et al. 2017). Also, the range of motion of shoulder and elbow joints were constrained to be $-20°$–$110°$, and $0°$–$170°$, respectively.

The impact of stroke on the neuro-musculoskeletal system was modeled by a set of coefficients that modify the significance of the muscle force in the process of finding the optimal motion. In other words, we assume that the neural connections from the CNS to the muscle are severed or affected by the stroke and this would scale the muscle stress s_i by coefficient c_i which is called Muscle Significance Factor (MSF) in this work. Equation (8) shows the affected muscle stress, $\hat{S}_i$, to be used in the cost function of the optimal control algorithm:

$$\hat{\mathbf{S}}(t) = \boldsymbol{diag}(\mathbf{C})\mathbf{S}(t) \tag{8}$$

where $\mathbf{S}(t)$ and $\hat{\mathbf{S}}(t)$ are the vectors of the muscle stress in a healthy and stroke subjects, respectively, $\mathbf{C}$ is the vector of MSF and $\boldsymbol{diag}(\mathbf{C})$ gives a diagnoal matrix with components of $\mathbf{C}$ on its main diagonal.

As a result, the determination of the subject-specific model consists of a two-tier optimization problem: A dynamic optimization problem is solved each time to calculate the motion trajectory of the model (the optimal controller or the CNS) for a given set of initial and final points. The numerical procedure is explained briefly in the next paragraph. The second optimization problem was formulated on the next level to obtain the MSF. This problem which will be detailed in Sect. 2.2.1, finds the optimum set of MSF that brings the model predictions for the motion trajectories as close as possible to the experimental ones.

In order to obtain the optimal trajectory, the Variation of Extremals (VE) approach (Kirk 2004) was used. The method is an iterative numerical technique to solve optimal control problems with known boundary conditions. In this problem, muscle stress is the cost function to be minimized while complying with the dynamic equations of the musculoskeletal arm model [Eq. (1)] and the boundary conditions on the initial and final positions of the arm.

2.2.1 Model parameter identification

Most of the model parameters were selected according to the anthropometric tables (Holzbaur et al. 2007; Murray et al. 2000; Nakano et al. 1999). The length of the upper and lower arm segments was measured directly from each subject.

The critical parameter in the proposed model is the MSF which needs to be experimentally determined for each stroke subject. According to the definition in Sect. 2.2, the cost func-

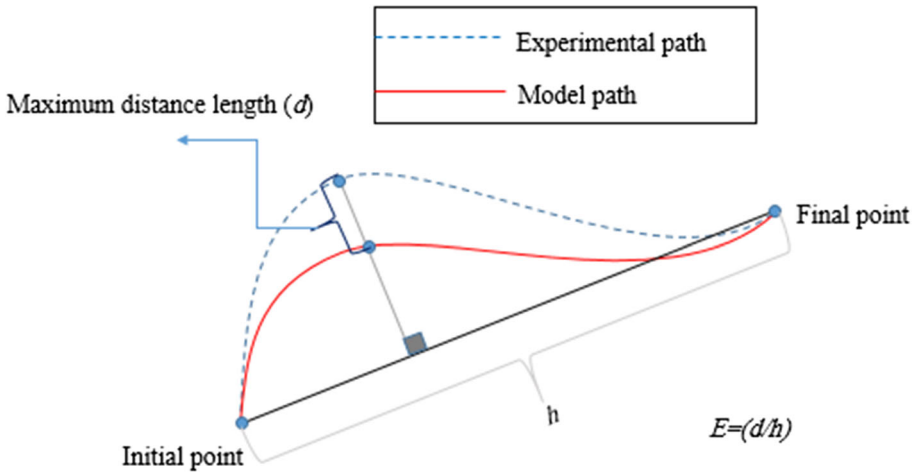

Fig. 3 A modified curvature index, E, is used to compare the geometry of the model generated path with that of the experiments

tion is a linear function of the MSFs. As a result, the scale of the MSF does not have any impact on the optimal solution and thus the CNS model performance. Therefore, the MSF was assumed to be between 0 and 1. In order to find the optimum values of MSF for each subject, an inverse optimization problem (Mombaur et al. 2010) was solved. In other words, the optimal values of the MSF, were determined such that they minimize the error between the patient's performance in a particular motion and the predicted path by the model. The details on how the error between the two paths were calculated are given in Sect. 2.3.

Particle Swarm Optimization (PSO) (Eberhart and Kennedy 1995) was used to solve the optimization problem. The method has been reported to have good performance in problems where the search space is continuous and the cost function evaluation has high computational cost. For our problem, we supposed 6 vectors as the swarm, each vector contained 6 coefficients for the MSF with randomly selected initial values. The search was stopped when error, E, was less than 0.5% or the search passed 30 iterations.

2.3 Error index

The comparison between the model predictions and the patient's motion can be done in three levels: (1) Path geometry, (2) Trajectory profile (i.e., velocity, acceleration.) and (3) Muscle forces. In the present work, as the first step, the comparison was performed on the path geometry.

Several error measures on the path geometry are presented and evaluated in (Bernabucci et al. 2007). The core concept in their proposed index is the difference between the curved path traveled by the arm versus the straight line connecting the initial and target points. Maximum Curvature Distance (MCD), for example, was defined as the maximum distance between the actual and straight paths divided by the straight path length. As a result, MCD compares the geometry of the actual path in a reaching task with a straight path assumed as the reference or the ideal one.

In this work, the MCD index was adopted from (Bernabucci et al. 2007) with minor modifications. The index was originally defined to compare a reaching arm motion in which a straight path is assumed as the reference. In this work, however, two general arm motions are to be compared where the straight path cannot be assumed as the ideal one. Therefore, as shown in Fig. 3, the largest distance between the two paths was first measured along a direction normal to the straight path. The error index, E, was then found by dividing the measured distance by the straight path length.

2.4 Experiments

Six stroke patients and two healthy subjects participated in this study. All stroke participants were male with 40–55 years of age with Brunnstrom levels of 4–6, and at least 6 months post-stroke. None of the participants had a significant cognitive impairment (i.e., Mini-Mental State Examination ≥ 23) (Mehdizadeh et al. 2015). Several motions were recorded from each subject, each motion was identified by an initial and a final point (See Fig. 4). Subjects were asked to move their hands from an initial point to a final one shown by markers on the table. The participants were asked to repeat each movement 4 times and the median was selected. The median of the four movements was the one that had the minimum sum of difference with all others. According to a previous study (Cirstea and Levin 2000), the reaching performance of the upper extremities in stroke patients is almost independent from the initial and target points as long as they are inside the reachable workspace of the subject's hand. As a result, in this study, the reachable space was determined for each subject and the target points were selected such that the path lies

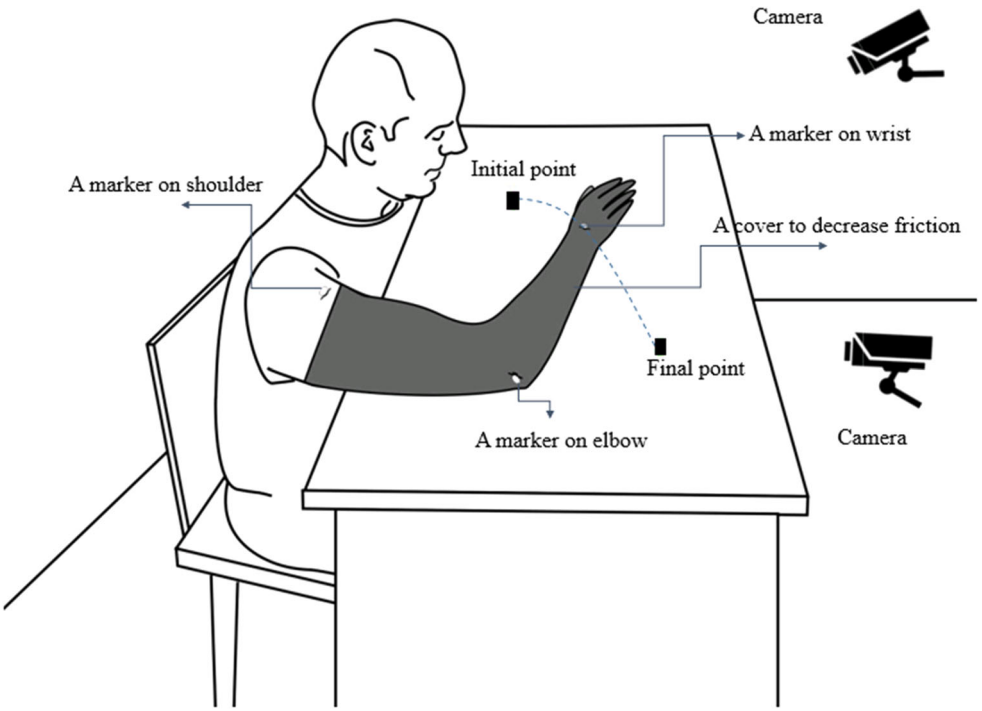

Fig. 4 A schematic of the experimental setup. The subject was seated on a straight-backed chair and moved his hand on a horizontal plane on the table from the initial point to the final one. The arm was covered by a long sleeve and glove to minimize the friction during the movements

inside and provide a relatively full coverage of the reachable space.

The participants were able to maintain their shoulder stationary and their wrist pronated with the palm facing down during the movements. Such stroke subjects have usually moderate to low stiffness in their joints (Macko et al. 2001), however, to ensure the stiffness and spasticity do not significantly impact the results, a correlation analysis was done between the Ashworth scale of muscle spasticity (Charalambous 2014) and their hand movement speed. A Pearson's coefficient of 0.43 was obtained which confirmed this assumption.

Details of the experimental setup are shown in Fig. 4. The participants' trunk was fixed to the chair as they sat at a raised table, so that their hand would move on a horizontal plane at the level of the shoulder. To minimize the friction between the hand and the table surface, the hand was covered by a long sleeve and glove. The patients were asked to rest their arm's weight on the table while performing the motions so the kinematics of the arm complies with the assumptions of the model. For the measurement of the hand movements, three markers were installed on the participant's arm: one marker on the wrist, another one on the elbow and the last one on the shoulder. The Cartesian coordinates of the markers were recorded using a Vicon™ (Shelbyville, Indiana, USA) motion capture system with a sampling frequency of 120 Hz.

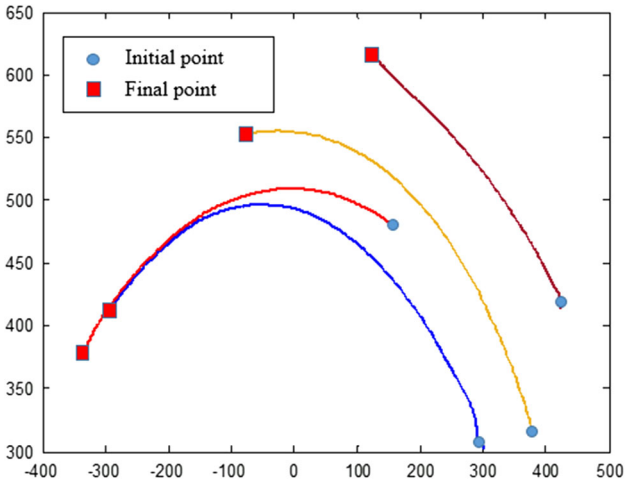

Fig. 5 A typical series of movements made by the left hand of a subject

3 Results

Figure 6 illustrates a typical series of movements performed by one subject. Each motion, identified by an initial point and a final one, was repeated four times and the median was selected and is shown in Fig. 5. The shoulder of the subject was considered as the origin of the coordinate system, the X-axis was along the shoulder line and the Y-axis pointing to the front.

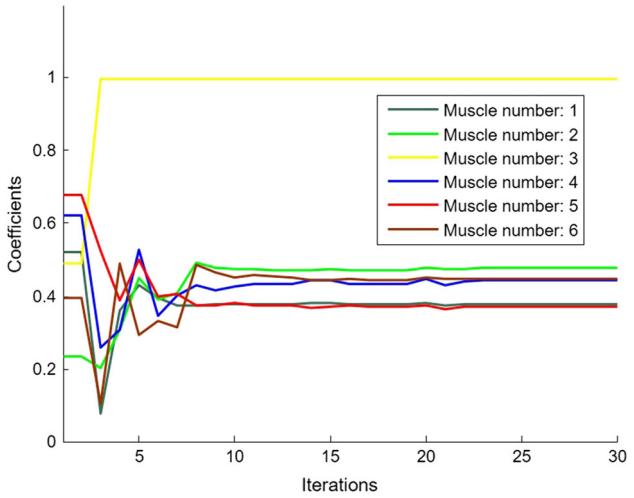

Fig. 6 Iterative search for the MSF of a subject based on one of his movements using the PSO technique. Each color shows the coefficient of a muscle (colour figure online)

The MSF for each subject was determined using the PSO technique as explained in Sect. 2.2.1. For a typical subject, the convergence of the MSF is shown in Fig. 6 which occurred after about 10 cycles.

In order to investigate the robustness of the MSF (its dependency on the motion), it was calculated based on four different motions of each participant. The results are shown in Fig. 7 in which, three typical subjects with Brunnstrom levels of 4, 5 and 6 are reported. Each diagram belongs to one subject. The values of MSFs for all six muscles from the model are shown by bar charts. Each pattern presents the MSF calculated based on a distinct motion. It is desired that the MSFs do not change significantly when found based on different motions.

For a more precise presentation on the robustness of the MSF, the mean values and maximum variations of the MSF for subjects of each Brunnstrom level are provided in Table 1. For each subject, the MSF was found using different motions. Then, the mean values and the maximum variations of each element (in percentage) were found. The maximum variation indicates how sensitive each element of the MSF is to the type of motion used for its calculation and therefore it is desired to be as small as possible.

The next set of results report on the healthy or unaffected subjects. As a control experiment, the MSF was calculated based on the motions of healthy subjects or the unaffected arm of the stroke subjects. According to the concept of MSF explained in Sect. 2.2, the values of MSF for a normal subject should be all about 1 indicating that the CNS has similar and complete access to all muscles while planning a motion. To investigate this, the MSFs were found for healthy and unaffected arm motions through the PSO optimization and 30 iterations. Then the standard deviation of each set of the MSF of each subject was calculated which are reported in Table 2. A lower standard deviation indicates that the MSF values for a subject are more uniformly distributed about the expected value of 1.

The evaluation of the proposed stroke model was done by comparing its predicted path of motion with that of the experiment in each subject. For this purpose, the MSF for the model of each subject was found from one of his motions. Then, the predicted path of the model for other recorded motions was found using the initial and final points. Figure 8 shows the model and the experimental results, for typical subjects from each Brunnstrom level (4, 5, and 6). Also, the model results before applying the MSF (i.e., healthy model) are shown in order to illustrate the effects of the MSF on making the model results similar to that of the stroke subjects. The accuracy of the model was measured by the same error index defined in Sect. 2.3. The results are presented in Table 3. Also, in order to show the variation of the results among the subjects in each Brunnstrom level, the mean and maximum variation of the error are reported in Table 4.

4 Discussions

The core purpose of this work was to propose a method to incorporate the stroke effects to the mathematical models of the arm motion. When stroke occurs, some neural connections between the CNS and the muscular system are severed. As a result, the CNS cannot stimulate and control all muscles as before. In the framework of an optimal control model for the CNS, the level of control on the muscles in post-stroke is incorporated by using the MSF (Muscle Significance Factor) in the cost function to determine the altered significance of each muscle in the motion planning. In other words, it is assumed that the CNS is still trying to find the optimum motion, however, the significance of individual muscles have been altered due to the stroke which results in different motion paths. In the following, different aspects of this idea are evaluated and discussed according to the model and the experiments carried out in this study.

First, it is seen from Fig. 6 that the convergence of the MSF was relatively fast and computationally affordable using a heuristic search method (PSO). For the biomechanical model consisting of six muscles and two links, determination of the MSF took between 30 and 180 s on a Core i7 Windows™ platform. This, however, may increase by the complexity of the model, i.e., the number of the involved muscle and the degrees of freedom.

The robustness of the MSF and the overall model accuracy in path prediction in stroke subjects are discussed in more details in the following.

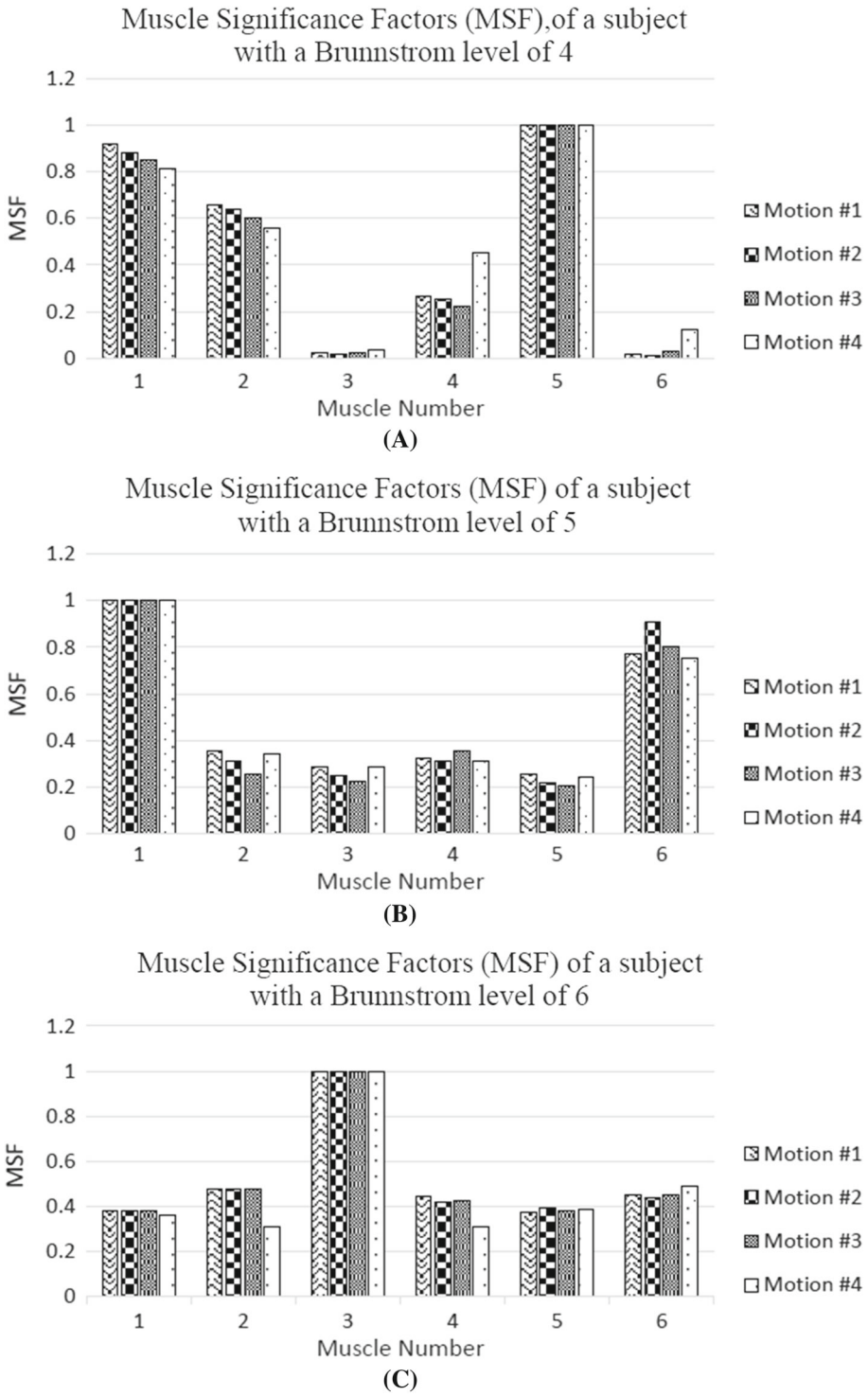

Fig. 7 The MSF of three subjects calculated based on four different motions to show the robustness of the MSF. Diagrams **a**–**c** Belongs to stroke patients with Brunnstrom levels of 4, 5 and 6, respectively

4.1 Robustness and uniqueness of the MSF

In order for the MSF to correspond to actual neurophysiology of the subject, they have to be independent from the arm motion by which they were found. The dependency of the MSF on the arm motion was analyzed based on the results shown in Fig. 8 and Table 1. Different sets of arm motions were used in the optimization procedure to calculate the MSF. The variations of the MSF for three typical subjects with Brunnstrom levels of 4, 5, and 6 are summarized in Table 1.

It is seen from Table 1 that the variation of the MSF for all three subjects is in the range of 0–2.58% with a mean value of 0.35%. This range for the subjects with Brunnstrom level of 5 and 6 is 0–0.35% with a mean of 0.17%. As a result, in

Table 1 The mean and maximum variation of MSF (four different motions were used)

Subject number	Brunnstrom level	Mean values of MSF	Maximum variation of MSF
1	6	[0.37, 0.42, 1, 0.39, 0.38, 0.45]	[0.05%, 0.4%, 0%, 0.35%, 0.05%, 0.1%]
2	6	[0.57, 0.74, 1, 0.42, 0.5, 0.55]	[0.1%, 0.32%, 0%, 0.04%, 0.42%, 0.33%]
3	5	[0.33, 0.48, 0.52, 0.32, 0.19, 1]	[0.05%, 0.4%, 0%, 0.35%, 0.05%, 0%]
4	5	[1, 0.31, 0.29, 0.32, 0.23, 0.8]	[0%, 0.32%, 0.24%, 0.13%, 0.22%, 0.16%]
5	4	[0.23, 0.57, 0.18, 0.48, 0.12, 1]	[0.62%, 0.13%, 0.81%, 0.29%, 1.88%, 0%]
6	4	[0.87, 0.61, 0.023, 0.30, 1, 0.04]	[0.13%, 0.17%, 0.73%, 0.76%, 0%, 2.58%]

Table 2 The standard deviation of MSF vector for the affected side, unaffected side and the healthy subjects

Subject number	Brunnstrom level	SD of MSF of the affected arm	SD of MSF of the unaffected arm
1	6	0.77	0.09
2	6	0.59	0.12
3	5	0.92	0.1
4	5	1.03	0.15
5	4	1.12	0.21
6	4	1.19	0.27
7	Healthy	–	0.085
8	Heathy	–	0.097

general, the dependency of the MSF on the motion is seen to be relatively minimal. This supports the hypothesis that the MSF is an intrinsic property of the post-stroke CNS and hence converges to a relatively unique set of values.

The variation in the MSF values, however, seems to slightly increase for lower Brunstrom levels in which the limb motions are more erratic.

The MSF of healthy subjects and the unaffected arm of stroke patients were calculated to see if the MSF can properly correlate with the neural damage or distinguish between the normal and affected arm motions. Since the MSF values indicate the presence and significance of the muscles in the optimal motion planning by the CNS, it is expected that in a healthy motion, the values of MSF have a uniform distribution. As seen in Table 2, the SD (standard deviation of the elements of the MSF) is at a minimum in healthy subject or on the unaffected side of the subjects. There is a significant increase in SD (about 5.5 times) comparing the unaffected side with the affected one which confirms our assumption.

4.2 Model accuracy

It is seen from Fig. 8 that using the healthy model to predict the hand motion of a stroke subject has poor accuracy which is substantially improved when the MSF is introduced to the neuro-musculoskeletal model. The healthy model, in all Brunnstrom levels, has a mean error of 22% when compared to the experimental data. This overall mean value of error was decreased to 2.73% when MSF was introduced to the model.

Table 3 presents the dependency of the model accuracy on the type of motion. The first motion of each subject is used to determine the MSF and therefore the model should have the least error for this motion as confirmed by this table. It is, however, seen that the model performance for other motions maintains a fair level of accuracy. In the worst case, the path error has changed from 0.5 to 6.8%. It was observed that the variation of error mostly depends on the length of motion and the stroke level. The error was seen to decrease by the length of motion. This may indicate that the initial and final moments of a motion are where the maximum error occurs which is also seen from the motion paths (Fig. 8). In the beginning of a motion, other neural functions such as cognitive abilities (e.g., attention) become substantial which are not included in this model. At the end of each path, the subject usually overshoots and then returns to the target point while this cannot occur in the optimally controlled path generated by the model.

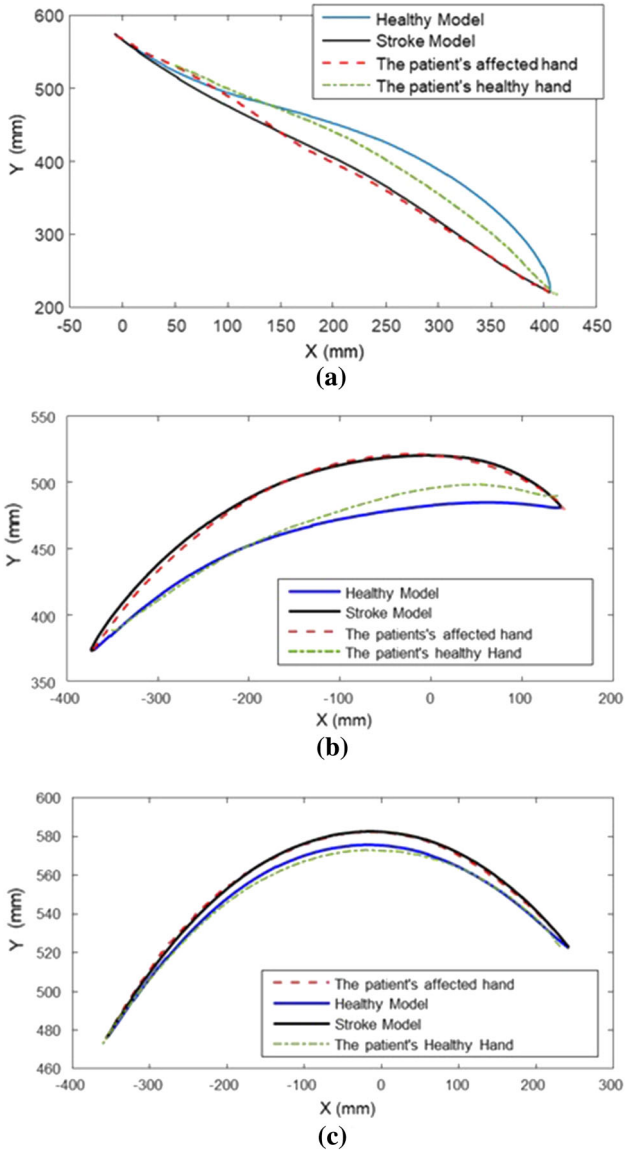

Fig. 8 The predicted path of motions by the stroke model versus the results of experiments. The dash-dot lines show the results of the model before using the MFS, the solid lines are the predicted movements by the stroke model, and dash lines show the experimental results. Parts **a**–**c** correspond to Brunnstrom levels of 4, 5 and 6, and patient number 7, 3, and 1, respectively

Table 3 The error between the predicted path by the stroke model and experiment

Subject number	Brunnstrom level	Model prediction error (%)			
		Motion #1	Motion #2	Motion #3	Motion #4
1	6	0.5	0.8	0.7	0.3
2	6	0.5	1.2	1.3	0.9
3	5	0.5	0.5	2	1.8
4	5	1.2	1.7	1.4	2.1
5	4	5.6	4.9	6.3	6.8
6	4	4.5	5.5	5.8	5.2

The MSF for each subject is determined using the first motion

Table 4 The mean and maximum variation of error for all patients of each Brunnstrom level (based on Table 3)

Brunnstrom level	Mean of error (%)	Maximum variation of error (%)
6	0.9	8.88
5	1.4	0.43
4	5.58	0.42

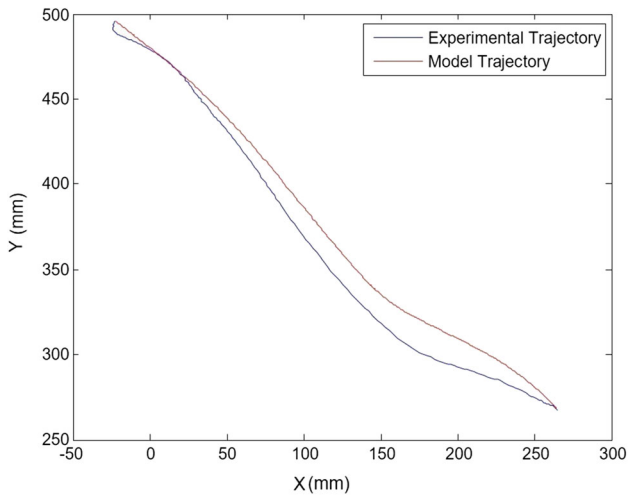

Fig. 9 Predicting an s-shaped path of a level 4 stroke subject by the model

The accuracy of the stroke model in motion prediction, seen from Table 4, is also dependent on the Brunnstrom level. For levels 5 and 6, the error was always less than 2.8%. The mean error of 1.73% and maximum variation of 1.35% indicate a fair agreement between the model and the stroke patients. However, this error, as expected, increased for the subjects of level 4. For level 4 of Brunnstrom, the mean of error was 5.58% with a maximum variation of 0.42% among the subjects of this level. This indicated that in lower levels, the impact of the neural damage on the motor control becomes more complex. Note that in level 3 or lower, the subject may not be able to perform the required motions and therefore, the proposed model is not applicable.

Comparing the model predictions and the experimental paths of motions, also indicated that the model provides a good prediction of the shape of the path. Note that the proposed error index only shows the maximum geometrical distance between the two paths. The path of hand motion for a post-stroke subject may not have the typical bell-shaped path of a normal subject. For instance, Fig. 9 shows the path of motion for a subject with a Brunnstrom level of 4. As

seen, the path has an s-shape. The model was also successful in predicting a similar s-shaped path.

4.3 Suggested future developments

Being the first step toward a model for post-stroke hand motions, in the experiments, the complexity was minimal. The pattern of motions was similar in the form of a circular arc. They all involved a shoulder abduction/adduction along with an elbow flexion/extension. The comparisons and model evaluations were also on the geometry of the motion. This can be further generalized using functional reach movements in which the direction of the movement, muscle synergies and actuation patterns are diversified. Also, comparisons between the velocity profiles, joint torques and muscle forces will extend the validity and hence application of the model.

5 Conclusions

The idea of Muscle Significance Factor, MSF, was evaluated and shown to be promising for incorporating the effects of neural damage caused by stroke to the optimal control model of arm motion. The hypothesis of this work was that the CNS, after stroke, still tries to optimize the muscle tensions while planning a path of motion. However, since the neural connections to some of the motor units are damaged, the outcome of the optimal motion differs from that of a normal person. This lack of full accessibility to muscles was incorporated into the model using a set of multipliers (MSF) which determine the relative significance of that muscle in the optimal control procedure. The MSFs were found using the kinematics of a typical motion of the patient and then incorporated into his model to predict the other motions. The procedure was shown to be robust meaning that the values of the MSFs are almost invariant to the subject's motion implying that they are intrinsic properties of the neuro-musculoskeletal system. The accuracy of the model in predicting the path of motion was also shown for 6 participating subject to be fair and comparable with similar models of healthy persons (Sharifi et al. 2017). The future works will include evaluation of the model in functional reach movements and also in velocity and force level.

Acknowledgements This work was partially supported financially by Iran National Science Foundation, under Grant Number 92042014.

Compliance with ethical standards

Ethical approval All procedures performed in studies involving human participants were in accordance with the ethical standards of the institutional and/or national research committee and with the 1964 Helsinki Declaration and its later amendments or comparable ethical standards.

Informed consent Informed consent was obtained from all individual participants included in the study.

References

Anderson FC, Pandy MG (2001) Dynamic optimization of human walking. J Biomech Eng 125:381–390

Balaghi E, Hadi M, Vatankhah R, Broushaki M, Alasty A (2016) Adaptive optimal multi-critic based neuro-fuzzy control of MIMO human musculoskeletal arm model. Neurocomputing 173:1529–1537

Bernabucci I, Conforto S, Capozza M, Accornero N, Schmid M, D'Alessio T (2007) A biologically inspired neural network controller for ballistic arm movements. J Neuroeng Rehabil 4:33

Bhushan N, Shadmehr R (1999) Computational nature of human adaptive control during learning of reaching movements in force fields. Biol Cybern 81:39–60

Blana D, Kirsch RF, Chadwick EK (2009) Combined feedforward and feedback control of a redundant, nonlinear, dynamic musculoskeletal system. Med Biol Eng Comput 47:533–542

Breteler MDK, Spoor CW, Van der Helm FCT (1999) Measuring muscle and joint geometry parameters of a shoulder for modeling purposes. J Biomech 32:1191–1197

Çelik G, Baykan ÖK, Kara Y, Tireli H (2014) Predicting 10-day mortality in patients with strokes using neural networks and multivariate statistical methods. J Stroke Cerebrovasc Dis 23:1506–1512

Charalambous CP (2014) Interrater reliability of a modified Ashworth scale of muscle spasticity. In: Classic papers in orthopaedics. Springer

Cirstea MC, Levin MF (2000) Compensatory strategies for reaching in stroke. Brain 123:940–953

Dong H, Figueroa N, El Saddik A (2015) Adaptive "load-distributed" muscle coordination method for kinematically redundant musculoskeletal humanoid systems. Robot Auton Syst 64:59–69

Eberhart R, Kennedy J (1995) A new optimizer using particle swarm theory. In: Proceedings of the sixth international symposium on micro machine and human science, 1995. MHS'95. IEEE, pp 39–43

Flash T, Hogan N (1985) The coordination of arm movements: an experimentally confirmed mathematical model. J Neurosci 5:1688–1703

Han CE, Arbib MA, Schweighofer N (2008) Stroke rehabilitation reaches a threshold. PLoS Comput Biol 4:e1000133

Heim A, Stryk OV (2000) Trajectory optimization of industrial robots with application to computer aided robotics and robot controllers. Optimization 47:407–420

Holzbaur KRS, Murray WM, Gold GE, Delp SL (2007) Upper limb muscle volumes in adult subjects. J Biomech 40(4):742–749

Kirk DE (2004) Optimal Control Theory: An Introduction. Dover Publications, Mineola

Lee LF, Narayanan MS, Kanna S, Mendel F, Krovi VN (2009) Case studies of musculoskeletal-simulation-based rehabilitation program evaluation. IEEE Trans Robot 25:634–638

Li W, Todorov E (2007) Iterative linearization methods for approximately optimal control and estimation of non-linear stochastic system. Int J Control 80:1439–1453

Macko RF, Smith GV, Dobrovolny CL, Sorkin JD, Goldberg AP, Silver KH (2001) Treadmill training improves fitness reserve in chronic stroke patients. Arch Phys Med Rehabil 82:879–884

Mehdizadeh H, Taghizadeh G, Ghomashchi H, Parnianpour M, Khalaf K, Salehi R, Esteki A, Ebrahimi I, Sangelaji B (2015) The effects of a short-term memory task on postural control of stroke patients. Top Stroke Rehabil 22:335–341

Mombaur K, Truong A, Laumond J-P (2010) From human to humanoid locomotion—an inverse optimal control approach. Auton Robots 28:369–383

Murray WM, Buchanan TS, Delp SL (2000) The isometric functional capacity of muscles that cross the elbow. J Biomech 33(8):943–952

Nakano E, Imamizu H, Osu R, Uno Y, Gomi H, Yoshioka T, Kawato M (1999) Quantitative examinations of internal representations for arm trajectory planning: minimum commanded torque change model. J Neurophysiol 81(5):2140–2155

Park H, Durand DM (2008) Motion control of musculoskeletal systems with redundancy. Biol Cybern 99:503–516

Pigeon P, Yahia LH, Feldman AG (1996) Moment arms and lengths of human upper limb muscles as functions of joint angles. J Biomech 29(10):1365–1370

Reinkensmeyer DJ, Iobbi MG, Kahn LE, Kamper DG, Takahashi CD (2003) Modeling reaching impairment after stroke using a population vector model of movement control that incorporates neural firing-rate variability. Neural Comput 15:2619–2642

Shadmehr R, Smith MA, Krakauer JW (2010) Error correction, sensory prediction, and adaptation in motor control. Annu Rev Neurosci 33:89–108

Sharifi M, Salarieh Ha, Behzadipour S (2017) Nonlinear optimal control of planar musculoskeletal arm model with minimum muscles stress criterion. J Comput Nonlinear Dyn 12:011014

Stroeve S (1998) Neuromuscular control model of the arm including feedback and feedforward components. Acta Psychol 100:117–131

Suzuki M, Yamazaki Y, Mizuno N, Matsunami K (1997) Trajectory formation of the center-of-mass of the arm during reaching movements. Neuroscience 76:597–610

Thaler L, Todd JT (2009) The control parameters used by the CNS to guide the hand depend on the visuo-motor task: evidence from visually guided pointing. Neuroscience 159:578–598

Todorov E, Jordan MI (2002) Optimal feedback control as a theory of motor coordination. Nat Neurosci 5:1226

Todorov E, Li W (2003) Optimal control methods suitable for biomechanical systems. In: Engineering in medicine and biology society, 2003. Proceedings of the 25th annual international conference of the IEEE. IEEE, pp 1758–61

Uno Y, Kawato M, Suzuki R (1989) Formation and control of optimal trajectory in human multijoint arm movement. Biol Cybern 61:89–101

Veeger HEJ, Yu B, An K-N, Rozendal RH (1997) Parameters for modeling the upper extremity. J Biomech 30(6):647–652

Zadravec M, Matjačić Z (2013) Planar arm movement trajectory formation: an optimization based simulation study. Biocybern Biomed Eng 33:106–117